Optical Diagnostics of Laser-Induced and Spark Plug-Assisted Hcci Combustion

Weinrotter, Martin; Wintner, Ernst; Iskra, Kurt; Neger, Theo; Olofsson, Jimmy; Seyfried, Hans; Aldén, Marcus; Lackner, Max; Winter, Franz; Vressner, Andreas; Hultqvist, Anders; Johansson, Bengt

Published in:
SAE Transactions, Journal of Engines

2005

Leading Our World In Motion

SAE TECHNICAL
PAPER SERIES

2005-01-0129

Optical Diagnostics of Laser-Induced and Spark Plug-Assisted HCCI Combustion

M. Weinrotter and E. Wintner
Photonics Institute, Vienna University of Technology

K. Iskra and T. Neger
Institute of Experimental Physics, Graz University of Technology

J. Olofsson, H. Seyfried and M. Aldén
Division of Combustion Physics, Department of Physics, Lund Institute of Technology

M. Lackner and F. Winter
Institute of Chemical Engineering, Vienna University of Technology

A. Vressner, A. Hultqvist and B. Johansson
Division of Combustion Engines, Department of Heat and Power Engineering

Reprinted From: Homogeneous Charge Compression Ignition (HCCI) Combustion 2005 (SP-1963)

ISBN 0-7680-1636-3

9 780768 016369

SAE International™

**2005 SAE World Congress
Detroit, Michigan
April 11-14, 2005**

400 Commonwealth Drive, Warrendale, PA 15096-0001 U.S.A. Tel: (724) 776-4841 Fax: (724) 776-5760 Web: www.sae.org

All SAE papers, standards, and selected books are abstracted and indexed in the Global Mobility Database.

ISSN 0148-7191

2005-01-0129

Optical Diagnostics of Laser-Induced and Spark Plug-Assisted HCCI Combustion

M. Weinrotter and E. Wintner
Photonics Institute, Vienna University of Technology

K. Iskra and T. Neger
Institute of Experimental Physics, Graz University of Technology

J. Olofsson, H. Seyfried and M. Aldén
Division of Combustion Physics, Department of Physics, Lund Institute of Technology

M. Lackner and F. Winter
Institute of Chemical Engineering, Vienna University of Technology

A. Vressner, A. Hultqvist and B. Johansson
Division of Combustion Engines, Department of Heat and Power Engineering

ABSTRACT

HCCI (Homogeneous Charge Compression Ignition), laser-assisted HCCI and spark plug-assisted HCCI combustion was studied experimentally in a modified single cylinder truck-size Scania D12 engine equipped with a quartz liner and quartz piston crown for optical access. The aim of this study was to find out how and to what extent the spark, generated to influence or even trigger the onset of ignition, influences the auto-ignition process or whether primarily normal compression-induced ignition remains prevailing. The beam of a Q-switched Nd:YAG laser (5 ns pulse duration, 25 mJ pulse energy) was focused into the centre of the cylinder to generate a plasma. For comparison, a conventional spark plug located centrally in the cylinder head was alternatively used to obtain sparks at a comparable location. No clear difference in the heat releases during combustion between the three different cases of ignition start could be seen for the fuel of 80/20 iso-octane/n-heptane used. However, with optical diagnostic methods, namely PLIF (Planar Laser-Induced Fluorescence), Schlieren photography and chemiluminescence imaging, differences in the combustion process could be evaluated.

INTRODUCTION

In an HCCI engine air and fuel are premixed and as the piston is reaching TDC (*T*op *D*ead *C*enter) the mixture auto-ignites at several locations simultaneously [1]. Since ignition occurs at multiple points, the integrated combustion rate becomes very high. Therefore, highly diluted mixtures or EGR (Exhaust Gas Recirculation) have to be used in order to limit the rate of combustion [2]. However, the big challenge with this combustion concept is auto-ignition timing control since this is only depending on pressure and temperature conditions at TDC. Combustion control can be done by adjusting operational parameters as inlet air temperature, fuel amount and EGR rate [3,4]. Normally, cycle to cycle variations in terms of IMEP (*I*ndicated *M*ean *E*ffective *P*ressure) are very low [5,6] in HCCI combustion but, with late combustion timing, cycle to cycle variations increase and the combustion becomes unstable. By using an additional heat source in form of a spark, either electrical or by a laser-induced plasma, advancement of the auto-ignition timing can be achieved [7]. The major advantages of HCCI mode compared to diesel engine operation are low NO_x emissions and, depending on the fuel, virtually no soot [8]. The benefit of HCCI compared to SI (*S*park *I*gnition) combustion is the much higher part load efficiency [9]. The toughest challenge is controlling the ignition timing over a wide load and speed range [10,11]. Another challenge is to obtain an acceptable power density. The power density is limited by combustion noise and high peak pressures. At low loads, the rather high emissions of unburned hydrocarbons and carbon monoxide, in combination with low exhaust temperatures, present an additional challenge [12]. By applying unthrottled HCCI combustion at part load in SI engines, efficiency can be improved by 40-100%. Emerging technologies for variable valve timing, with the intent of using these as a means of controlling the combustion timing in HCCI engines [13],

may well lead the way for the first application of the HCCI combustion mode in practice.

In this work, HCCI combustion was either combined with a well-timed laser-induced plasma generated by a short laser pulse (5 ns) or a conventional spark plug ignition inside a combustion chamber of a six cylinder internal combustion engine. To overcome the difficulties of controlling the ignition timing an attempt was made to trigger HCCI combustion by spark plug or laser-induced ignition and observe this process by different optical diagnostic methods. PLIF, Schlieren photography and chemiluminescence imaging were applied. This work is a continuation of the work of Kopecek et al. [7] where the concept of a “laser triggered HCCI combustion” was proven. In the experiments presented the transition of spark ignition to auto-ignition should be analyzed.

A 10 mm NGK CR7E motorcycle spark plug and a Q-switched Nd:YAG solid-state laser have been used as alternative ignition sources. The focused short laser pulse leads to non-resonant breakdown [14] in the focal area followed by the formation of a hot dense plasma starting the combustion process. Such laser-induced plasmas are capable to ignite combustible mixtures like reported first by ref. [15]. Laser ignition offers several advantages in comparison to conventional spark plug ignition, like the ability to ignite leaner mixtures, arbitrary positioning of the ignition location and the potential of reduced service demand when applying monolithic, diode-pumped solid-state lasers. Highly developed spark plugs for stationary gas engines have a lifetime between 2,000 - 4,000 h in comparison to a laser ignition system with lifetimes of about 10,000 h. Further on, the ignition delay and overall combustion time are shorter and multi-point ignition can be applied more easily to enhance the combustion properties of ultra-lean mixtures [16,17].

The first experiments concerning a laser-ignited internal combustion engine were done by [18], demonstrating successful operation at leaner mixtures than being possible using conventional spark plugs. Furthermore, a natural gas engine was successfully operated in SI mode by a Q-switched laser running for a first test period of 100 hours without any interruption due to window fouling or other disturbances [19]. Also laser ignition and its advantages with respect to the potential future fuel hydrogen have been already investigated by [20]. A modified conventional gasoline engine was run by [24] on a daily basis including cold starts for over 200 hours. In recent experiments a 6 mm diameter entrance window and a much smaller and simplified laser system like the one described in this work was used. Preliminary results show reasonable reliability and motivate further investigation and development of laser ignition systems.

EXPERIMENTAL SETUP

ENGINE

The engine used for the tests was an inline six-cylinder Scania D12 diesel engine, converted to HCCI operation by using port fuel injection. The engine worked in single cylinder operation and optical access was enabled by a quartz liner and a quartz piston crown. The combustion chamber was of a disc shaped design and the compression ratio was chosen to be 11.2:1 for optimal optical access. A water cooled Kistler pressure transducer, placed 50 mm from the centre of the bore axis, was used for in-cylinder pressure capture. A photo of the engine can be seen in Fig. 1 and some vital engine specifications of the Scania D12 are shown in Table 1.

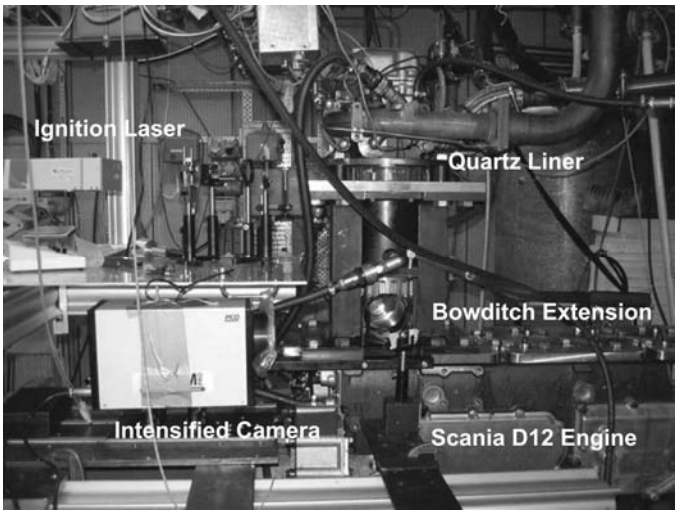

Figure 1: The modified Scania D12, the engine used for all the experiments conducted.

Displaced volume	*1966 cc*
Stroke	*154 mm*
Bore	*127.5 mm*
Connecting rod	*255 mm*
Compression ratio	*11.2:1*
Exhaust valve open	*34° BBDC @ 0.15 mm lift*
Exhaust valve close	*6° BTDC @ 0.15 mm lift*
Inlet valve open	*2° BTDC @ 0.15 mm lift*
Inlet valve close	*31° BBDC @ 0.15 mm lift*
Valve lift exhaust	*14.1 mm*
Valve lift inlet	*14.1mm*

Table 1: Technical specifications of the Scania D12 engine.

The inlet air was preheated by an electrical heater to initiate HCCI combustion with the selected compression ratio and fuel type. The experiments on the engine were conducted under the operating conditions shown in

Table 2. An air/fuel ratio of λ = 2.9 seemed to be the lean limit for successful combustion timing advancement using either spark formation method. The rich limit was limited by too rapid combustion and high in-cylinder pressures. The engine load for λ = 2.8 was 2.8 bar and for λ = 3.1 2.4 bar (IMEP). Due to high heat transfer to metal and glass parts at high load, adjustments of the inlet air temperature in the range of 2 °C had to be made in order to keep the combustion phasing constant.

Engine speed	*1200 rpm*
Lambda (λ)	*2.7 - 3.2*
Inlet air temperature	*175 - 200°C*
Inlet air pressure	*1 bar absolute*
Fuel	*80% Iso-octane and 20% n-heptane*

Table 2: Operational parameters of the engine.

IGNITION LASER

A Q-switched, flashlamp pumped Nd:YAG solid-state laser was employed to generate a plasma inside the combustion chamber of the engine for each cycle. Details and pulse energy can be found in Table 3. The laser pulse could be released at arbitrary crank angle positions and any rotation speeds by applying a special trigger interface. However, normally the speed was kept constant at 1200 rpm during the whole measurement requiring a constant pulse repetition rate of 10 Hz. A three-lens system (Extension-(1), collimating-(3), focusing-lens (4)) focused the beam through a quartz liner into the center of the cylinder, about 1 mm below the cylinder head (see Fig. 2). An additional cylindrical lens (2) had to be employed to compensate the effect of the quartz liner. A schematic drawing of the experimental setup with the ignition laser can be seen in Fig. 3.

Type	*Nd:YAG*
Wavelength	*1064 nm*
Pulse duration	*5 ns*
Pump source	*Flashlamp*
Pulse energy applied	*25 mJ*

Table 3: Specifications of the laser employed

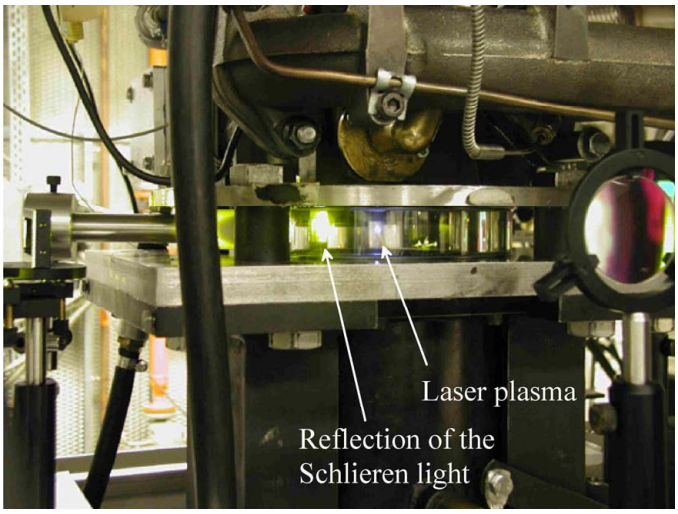

Figure 2: Blue laser plasma in the center of the figure with yellow Schlieren light

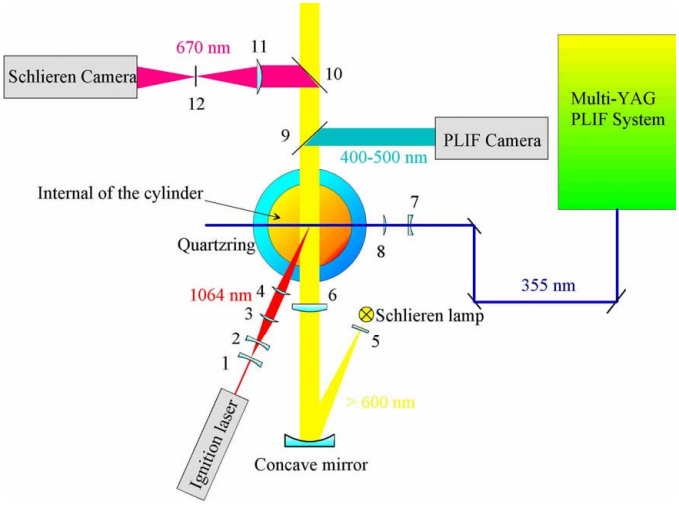

Figure 3: Experimental setup I; Schlieren / PLIF (vertical laser sheet): 1-Extension lens, 2-Cylinder lens(Ignition laser), 3-Collimating lens, 4-Focusing lens(f=100mm), 5-Filter (long pass cutoff 600nm), 6-Cylinder lens (Schlieren), 7-Cylinder lens (PLIF), 8-Focusing lens (PLIF), 9-Beamsplitter (reflecting 400-500nm), 10-Beamsplitter (reflecting 670nm), 11-Focusing lens (Schlieren), 12-Schlieren aperture (Knife-edge)

SCHLIEREN IMAGING

Schlieren photography was conducted in the plane of the focal spot of the igniting laser or the spark plug. As the index of refraction in gases is strongly dependent on density, areas with gradients of temperatures or pressures have considerable effect on the propagation of light. As a consequence, the refraction angle is proportional to the first derivative of these parameters. The experimental setup I is depicted in Fig. 3. Collimated light from a high pressure Mercury discharge lamp was directed through the combustion chamber. The focusing lens (11) has two functions: i) it focuses the unscattered part of the incoming parallel light and ii) it images a real and inverted picture of the scattered light on the CCD chip of an intensified camera. Now the parallel part of the beam is cut out by placing an aperture (12) in the focal region in a way that it covers

the focused light but enables the scattered part to pass around the focal area. Hence, regions with high temperature or pressure refract the parallel light and it can pass the aperture. To compensate the negative cylindrical lens effect of the quartz liner providing optical access to the engine, a compensating positive cylindrical lens (6) was inserted in the beam path before the cylinder. The difficulties due to engine motion, restricted optical access and distortion resulted in a somewhat reduced image size and quality, but nevertheless the effect of laser ignition on the onset of combustion could be clearly observed.

CHEMILUMINESCENCE IMAGING

Chemiluminescence imaging was performed by viewing through the quartz of the piston crown and a 45° mirror using the Bowditch extension scheme (see Fig. 1). A schematic drawing of the experimental setup II can be found in Fig. 4. The imaging system consisted of an intensified camera system equipped with UV optics and a dielectric coated beamsplitter (13), reflecting chemiluminescence emission around 308 nm while allowing passage for the fluorescence light of formaldehyde lying in the spectral range 400 nm and longer. The chemiluminescence images were recorded with an exposure time of 100 µs (0.72 CAD (*C*rank *A*ngle *D*egree)) unless otherwise stated. Spectral investigation of the emitted radiation revealed a distinct signature around 308 nm originating in the A-X emission band of OH and a broad underlying unstructured spectrum which can be attributed to carbon monoxide. Therefore, the images reveal not the exact location of the flame front but give a good overview of the occurence and development of flame kernels in the HCCI combustion process.

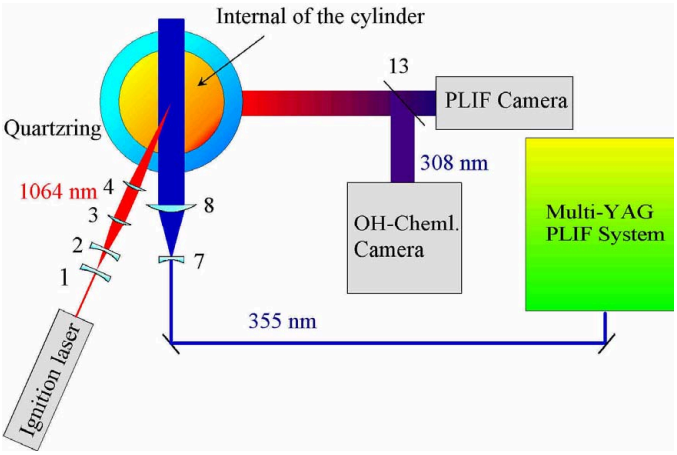

Figure 4: Experimental setup II; Chemiluminescence / PLIF (horizontal laser sheet): 1-Extension lens, 2-Cylinder lens (Ignition laser), 3-Collimating lens, 4-Focussing lens (f=100mm), 7-Cylinder lens (PLIF), 8-Focussing lens (PLIF), 13-Beam splitter (reflecting 308nm)

PLIF IMAGING

In order to capture the rapid combustion features in HCCI combustion, a high-speed imaging system was used. The formaldehyde LIF measurements were performed using a multi-YAG laser system. It consists of a cluster of four individual Q-switched Nd:YAG lasers with a fundamental wavelength of 1064 nm. The laser beams are frequency-doubled to 532 nm, combined with the neighboring beams by means of dichroic mirrors, and effectively frequency-tripled to yield a wavelength of 355 nm by sum frequency generation of the fundamental and the second harmonic. Eventually the four beams are aligned into a single optical output to be used in the experiments. By opening the Q-switch twice during one flashlamp discharge each laser can produce a double pulse, allowing a total of eight laser pulses to be fired in a rapid sequence. When operating in this fashion, the time separation between two consecutive pulses can be set to values as short as 6.25 µs. This short time-separation enables cycle-resolved LIF measurements, and provides sufficient temporal resolution for resolving the characteristic time scales in the turbulent environment of the HCCI engine.

In order to detect the LIF signal from the rapid laser pulses, a high-speed framing camera was used. In front of the optical input of the camera an f = 100 mm camera lens was mounted. Behind the optical input an eight-facet pyramid beam splitter directs the light onto eight individual intensified CCD modules. Each CCD module employs a 576 times, 384 pixel array with an 8 bit dynamic range, and an MCP (*M*icro *C*hannel *P*late) for exposure gating and signal intensification. The gating of each MCP is individually programmable and was synchronized with the laser pulses. In order to increase the overall sensitivity of the detection system an additional image intensifier was placed between the camera lens and the eight-facet prism. By using this intensifier unit, the minimum time separation between two consecutive images can be increased to 1 µs. However, this is not a limitation in the present application. For a detailed description of the laser/detector system, the reader is referred to [21-23].

For the formaldehyde LIF visualization the laser beam from the multi-YAG cluster was formed into a laser sheet by a combination of cylindrical (7) and spherical lenses (8) and directed into the combustion chamber of the HCCI engine via the quartz liner. To gain more thorough spatial information of the formaldehyde distribution, two different measurements were performed. The first setup (experimental setup I) included a laser sheet perpendicular to the cross section of the engine cylinder (see Fig. 3). In this case the fluorescence was imaged at a right angle through the quartz liner onto the framing camera. The second setup (experimental setup II) used a laser sheet in the cross sectional plane of the cylinder, and the fluorescence signal was imaged through the quartz piston via a UV enhanced 45° mirror in the piston extension onto the high-speed camera (see Fig. 4). In all LIF measurements performed, the time separation

between two consecutive images was set to 70 μs corresponding to 0.5 CAD of the engine. In front of the camera lens a long-pass filter with a cut-off wavelength of 385 nm was mounted, eliminating scattered laser light at 355 nm and transmitting the formaldehyde fluorescence. Since a small fraction of laser radiation at 532 nm from the frequency doubling process may still remain in the laser beam, an additional short-pass filter with a cut-off wavelength at 500 nm was used.

In the picture series the bright areas correspond to formaldehyde which is produced during the cool flame stadium prior to full compression some 20 CAD BTDC (*B*efore *T*op *D*ead *C*entre). The dark areas are depicting a consumption of formaldehyde which can be described as the burned regions in the mixture.

RESULTS AND DISCUSSION

The stabilizing effect of laser ignition has previously been reported by Kopecek et al. [7] using methane as fuel for HCCI combustion. The aim of this work was to get an insight into the mechanism of different supporting ignition sources on the onset and development of the combustion process by using a fuel which is more closely related to automotive applications. As n-heptane yields a good signal for formaldehyde PLIF diagnostics, a mixture of 80 % isooctane and 20 % n-heptane was chosen. The authors also tried a 50/50 % mixture yielding, however, no effect in combination with any ignition source (laser, spark plug) because of the too low octane number.

In unsupported HCCI, the mixture ignites at several spots throughout the compressed volume. Ignition timing and location are determined by the temperature and pressure history and the degree of inhomogeneity of the mixture. The concept of flame front propagation seems to loose its validity, leading to the term “controlled knock” for HCCI. Therefore, the idea of supporting HCCI ignition by additional spark plug or laser plasma ignition is not as straightforward as it seems.

UNSUPPORTED HCCI

A sequence of pictures recorded by PLIF imaging with vertical laser sheet (experimental setup I) during one particular cycle can be seen in Fig. 5. The pictures reveal the multipoint flame development structure during a combustion sequence. In all picture sequences of unsupported HCCI the formaldehyde consumption, which can be taken as a marker of the starting combustion, begins near the cylinder walls (left and right side of the pictures) like it can be observed in Fig. 5.

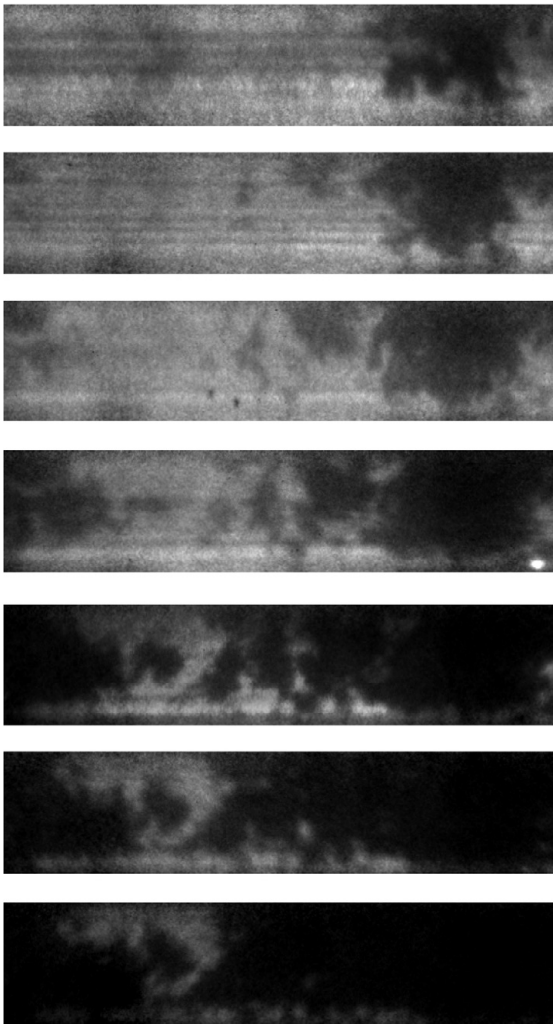

Figure 5: PLIF picture sequence; unsupported HCCI; vertical laser sheet (experimental setup I); λ = 2.8; first picture at 11.4° CA ATDC (After Top Dead Center); interval 0.5° CA; image size: 1.2 x 5.4 cm

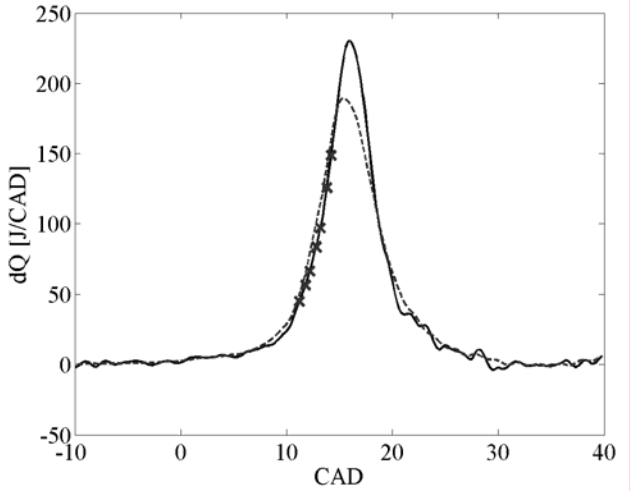

Figure 6: Heat release; unsupported HCCI; λ = 2.8; solid line corresponds to the PLIF picture series in Fig. 5; dots indicate the CAD when the PLIF pictures are taken; dashed line: average of 100 cycles, 50 taken before and 50 after the heat release indicated by the solid line

Fig. 6 shows the corresponding heat release (solid line) to the PLIF picture sequence in Fig. 5 measured during one cycle. The dots on the solid line indicate the CAD when the PLIF pictures were taken. The dashed line shows the average heat release of 100 cycles; 50 cycles before the heat release for the PLIF pictures (solid line) was taken and 50 cycles after. The COV IMEPnet was 0.21 bar and the COV in terms of CA50 was 3.20 CAD thus the cycle to cycle variations were large. As a result of this no clear difference in combustion characteristics (combustion timing, maximum pressure,…) could be observed between unsupported-, laser assisted- and spark plug-assisted HCCI combustion mode.

The resulting density and temperature gradients throughout the volume cause the even more grainy structure in the Schlieren image presented in Fig. 7. The used Schlieren camera was only able to take one picture per cycle. So the images were recorded one by one for every cycle, shifting the timing with a minimum interval of 0.5 CAD between the consecutive images. The images of the Schlieren setup cover a region of approximately 2 x 2 cm including the location of the spark plug and the laser plasma, respectively.

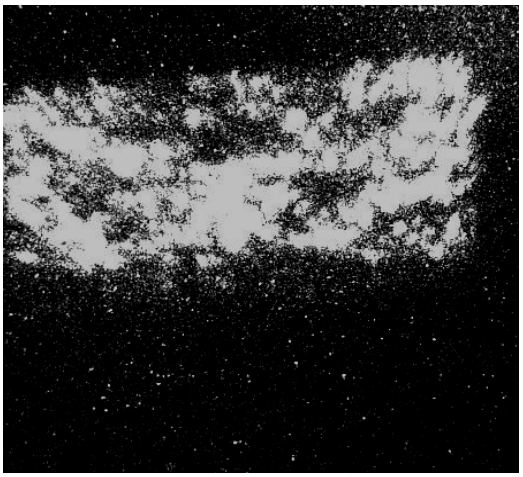

Figure 7: Schlieren picture; unsupported HCCI; (experimental setup I); λ = 2.8; image size: 2 x 2 cm; at 13° CA ATDC

Fig. 8 shows a PLIF picture sequence viewed through the quartz piston crown via the 45° mirror, like depicted in the experimental setup II in Fig. 4 applying a horizontal PLIF laser sheet. Hence these pictures are perpendicular to the ones in Fig. 5. Again, it can be seen that the combustion (formaldehyde consumption, dark regions) starts near the cylinder walls and proceeds through the unburned mixture.

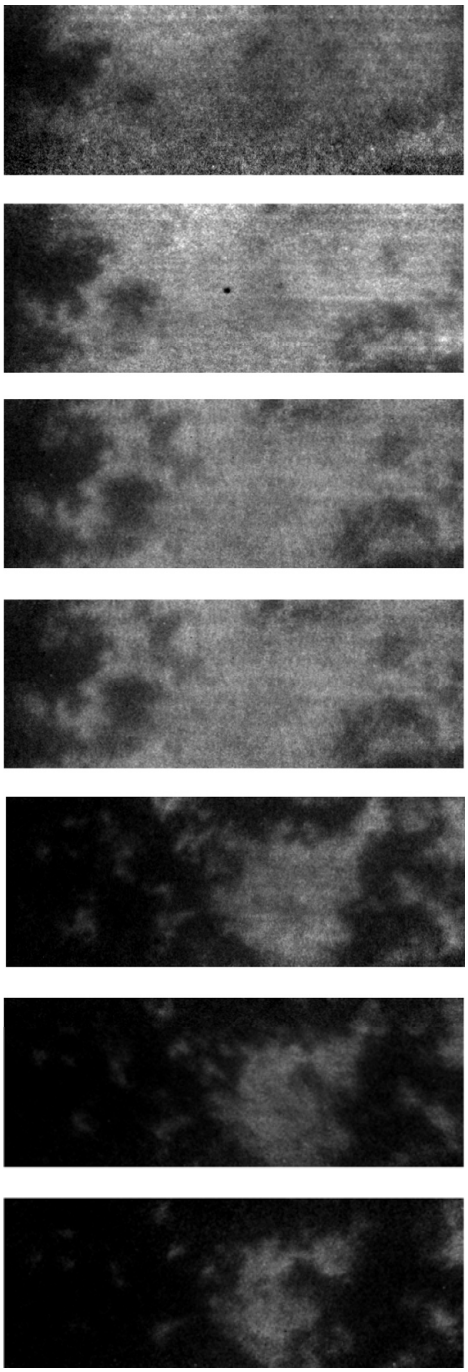

Figure 8: PLIF picture sequence; unsupported HCCI; horizontal laser sheet (experimental setup II; λ = 2.8; first picture at 11.4° CA ATDC; interval 0.5° CA; image size: 3.5 x 9 cm

Through the beamsplitter (13 in Fig. 4) it was possible to take chemiluminescence pictures at the same time like the PLIF pictures were taken as shown e.g. in Fig. 8. In Fig. 9, the whole combustion area can be seen from the bottom via the 45° mirror. The pictures are yielding just averaged intensity information over the line of sight (i.e. the vertical axis of the cylinder). The combustion starts at some points mostly close to the wall like in the PLIF pictures (Fig. 8), but the exact locations show erratic behavior from cycle to cycle. Consecutively, flame development starts at more and more points until the whole mixture is consumed. Both, the arbitrary locations

of ignition and the fast heat release typical for HCCI are clearly visible in these sequences.

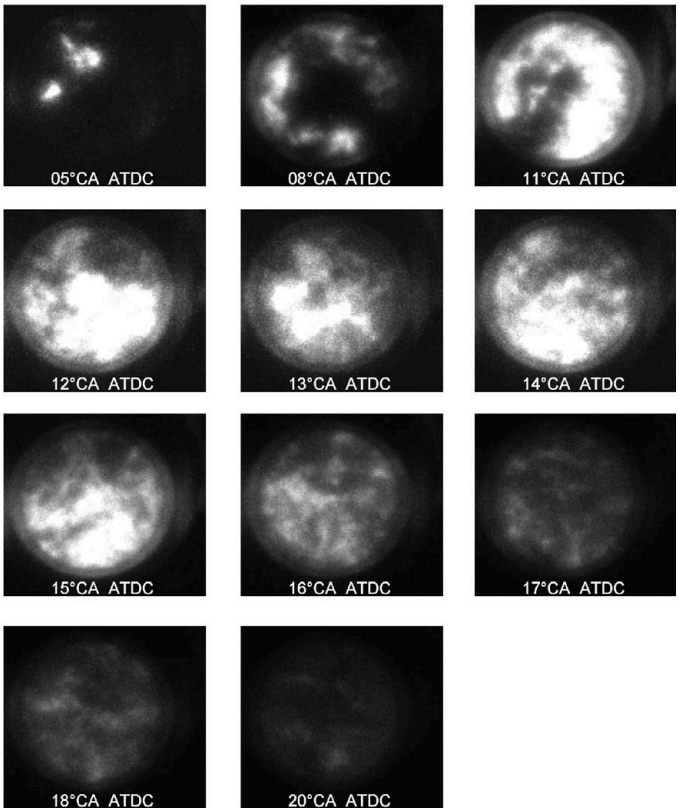

Figure 9: Chemiluminescence pictures (308 nm); unsupported HCCI; (experimental setup II); image size: 14 x 14 cm; λ = 2.8

LASER-ASSISTED HCCI

The second part of the experiments involved HCCI combustion for which starting was attempted by a laser-induced plasma at 25° CA BTDC. Earlier ignition timing was also tested, but no effect could bee seen in the images. The laser pulse energy was about 25 mJ and the pulse length was 5 ns. The air/fuel equivalence ratio λ had the value 2.8. With leaner mixtures than λ = 2.8 no effect of the laser or spark plug ignition could be seen.

Fig. 10 depicts a PLIF picture sequence with a vertical laser sheet (experimental setup I). In contrast to the unsupported HCCI case in Fig. 5, a clear “flame front” structure can be seen, which can be attributed to be caused by the ignition plasma. This effect of the laser plasma on the onset of combustion was not as pronounced at all cycles. The PLIF pictures showed all degrees of influence of additional ignition from strong flame front propagation to no effect at all. This erratic behavior is a result of a high COV (*C*oefficient *o*f *V*ariation) value like mentioned above and obscured the effect of laser ignition in the rate of heat release curves. Two reasons might contribute to these somewhat faint results: The ignition timing of the laser was too early, a fact determined by the limits of optical access. This problem could be overcome by using a laser entrance window in the cylinder head which was not available at that time. And the second feature unfavorable for pronounced supported ignition is the low octane number of the fuel used in these experiments. More appropriate fuels would be pure isooctane or gasoline for these test conditions. On the other hand these fuels would be a bad choice for the PLIF experiments due to the absence of formaldehyde.

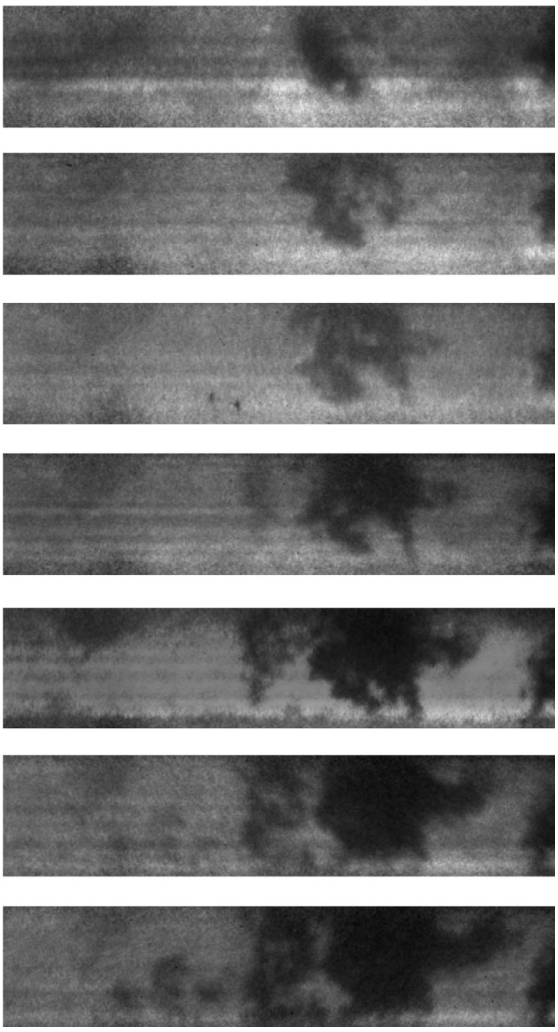

Figure 10: PLIF picture sequence; laser-assisted HCCI; vertical laser sheet (experimental setup I); λ = 2.8; first picture at 11.4° CA ATDC; interval 0.5° CA; ignition time: -25° CA BTDC; image size: 1.2 x 5.4 cm

The corresponding heat release (solid line) to the above depicted PLIF picture sequence can be found in Fig. 11. Like in Fig. 6, the dots on the solid heat release indicate the CAD when the PLIF pictures were taken. The dashed line shows the average heat release of 100 cycles; 50 cycles before the heat release for the PLIF pictures (solid line) was taken and 50 cycles after. The COV IMEPnet was 0.05 bar and the COV in terms of CA50 was 1.66 CAD.

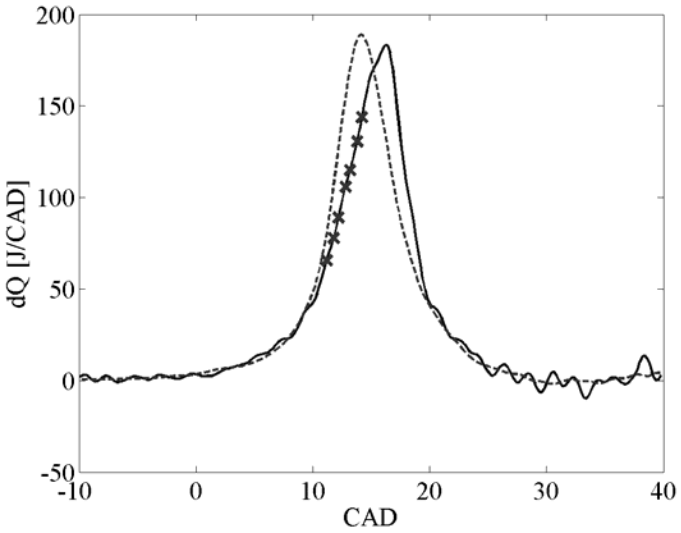

Figure 11: Heat release; laser-assisted HCCI; λ = 2.8; ignition time: -25° CA BTDC; solid line corresponds to the PLIF picture series in Fig. 5; dots indicate the CAD when the PLIF pictures are taken; dashed line: average of 100 cycles, 50 taken before and 50 after the heat release indicated by the solid line

The PLIF picture sequence in Fig. 12 taken through the quartz bottom piston via the 45° mirror shows again like the PLIF pictures in Fig. 10 an expanding "flame front" structure. In addition to that, also "normal" HCCI combustion starts from the left cylinder wall.

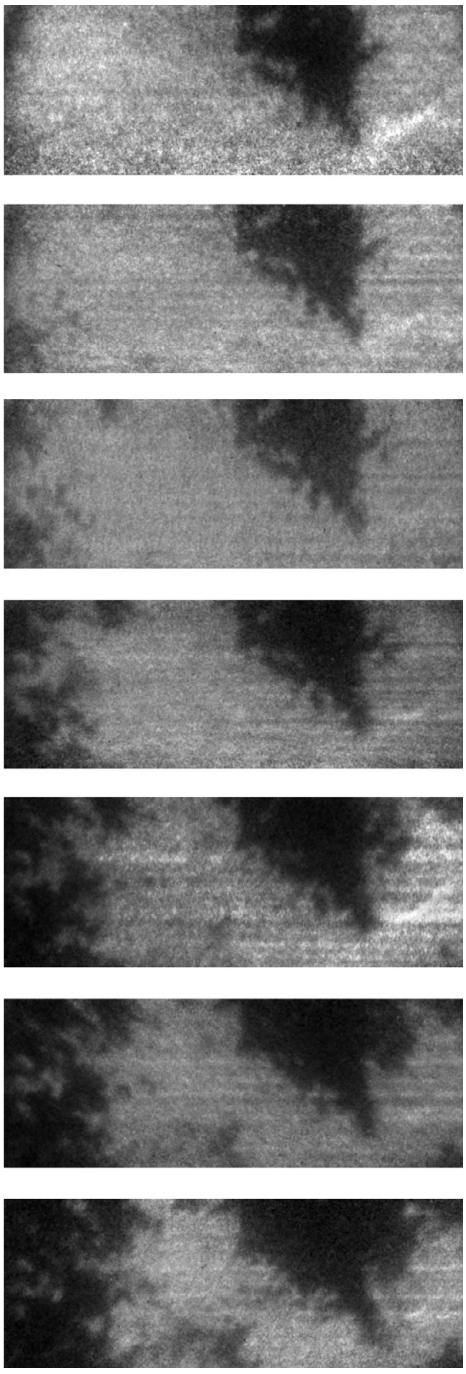

Figure 12: PLIF picture sequence; laser-assisted HCCI; horizontal laser sheet (experimental setup II); λ = 2.8; first picture at 11.4° CAD ATDC; interval 0.5° CA; ignition time: -25° CA BTDC; image size: 3.5 x 9 cm

In the chemiluminescence pictures in Fig. 13 viewed through the quartz piston, also some kind of flame front can be observed. In comparison to the unsupported HCCI combustion case in Fig. 9 where the combustion starts mainly near the cylinder walls, in these images an intensity peak can be observed in the middle of the cylinder. But it has to be pointed out that these pictures are taken from different cycles because the used intensified camera was only able to take one picture in a cycle.

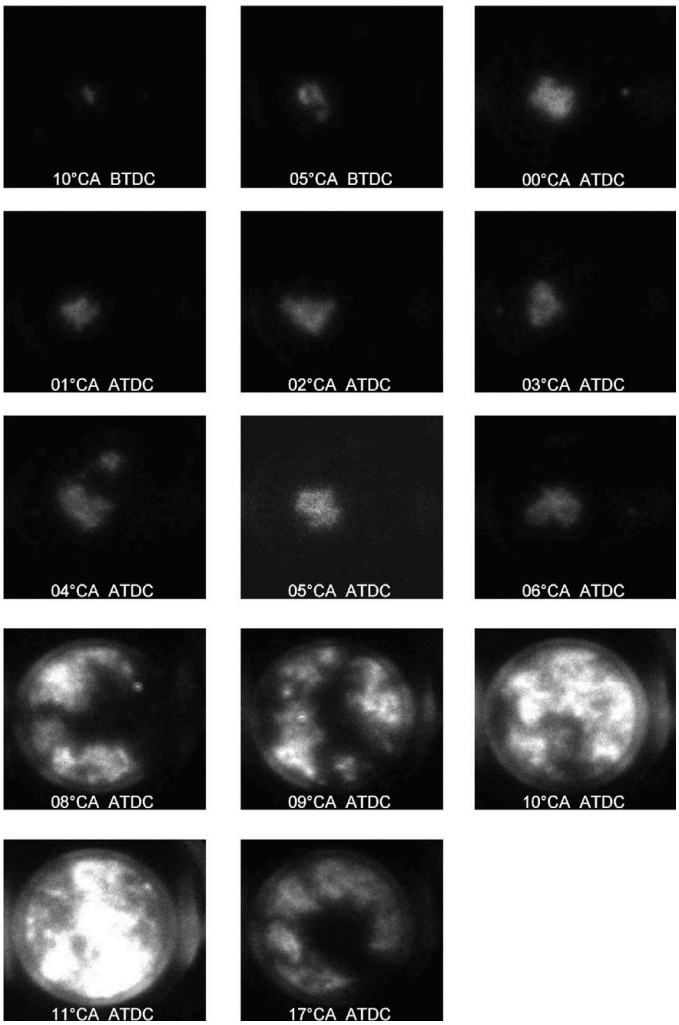

Figure 13: Chemiluminescence pictures (308 nm); laser-assisted HCCI; (experimental setup II); image size: 14 x 14 cm; λ = 2.8; ignition time: -25° CA BTDC

Fig. 14 shows Schlieren pictures through the quartz liner (experimental setup I). Again, it has to be taken into account that just one picture per cycle could be taken. One can see the growing combustion volume when the piston is going down from 0 to 20 CAD ATDC. But also in the Schlieren pictures it can be observed that the combustion is starting mainly from the middle of the combustion chamber in comparison to unsupported HCCI were the combustion starts mostly near the cylinder walls.

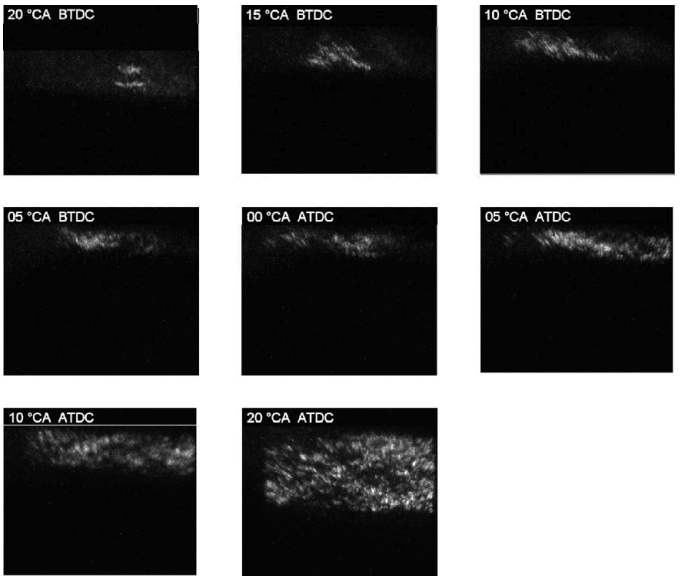

Figure 14: Schlieren pictures; laser-assisted HCCI; (experimental setup I); image size: 2 x 2 cm; λ = 2.8; ignition time: -25° CA BTDC

Cycle to cycle variations between corresponding images recorded at the same CAD were quite large. However, PLIF image sequences recorded during one cycle suggest that a Schlieren series would show similar flame front like behavior but requires an additional expensive multiexposure camera system, if one wants to compare both methods. The Schlieren images were considered illustrative and informative as well, but including all corresponding images from unsupported and spark plug assisted HCCI was omitted for brevity.

SPARK PLUG-ASSISTED HCCI

Beside laser-assisted HCCI also spark plug-assisted HCCI was investigated. The spark plug was positioned in the center of the cylinder head. The ignition timing was the same as for the laser-assisted case (25° CA BTDC) and the same air/fuel equivalence ratio of 2.8 was used. Like in the laser-assisted case, no effects of the spark in the images could be found if an earlier ignition time was chosen.

Again something like an “expanding flame front structure” can be seen in the PLIF picture sequence with the vertical laser sheet (experimental setup I) in Fig. 15. No big difference to the laser-assisted HCCI combustion case in Fig. 10 could be observed. But again as a result of a big COV-value sometimes nearly no effect of the spark could be observed and sometimes it was possible. The same behavior for the spark plug-assisted HCCI can be found in the chemiluminescence pictures in Fig. 16.

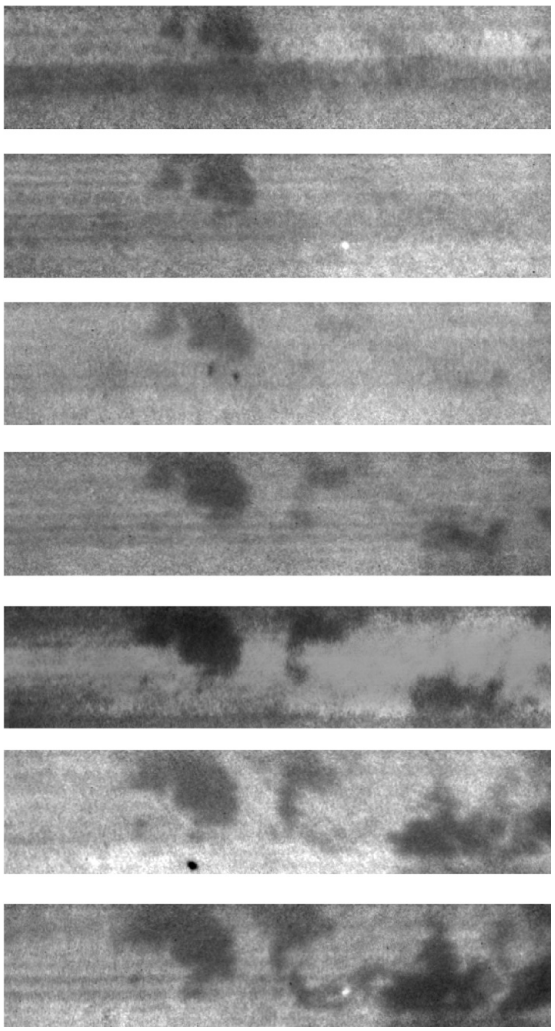

Figure 15: PLIF picture sequence; spark plug-assisted HCCI; vertical laser sheet (experimental setup I); λ = 2.8; first picture at 11.4° CA ATDC; interval 0.5° CA; ignition time: -25° CA BTDC; image size: 1.2 x 5.4 cm

Finally the heat release of the spark plug-assisted HCCI combustion is depicted in Fig. 17. Again, like in the other cases large cycle to cycle variations were present. The COV IMEPnet was 0.27 bar and the COV in terms of CA50 was 3.01 CAD. Hence, the conclusion of the heat release datas is that the COV was too big so no clear difference in the combustion characteristics of the three different combustion modes can be extracted.

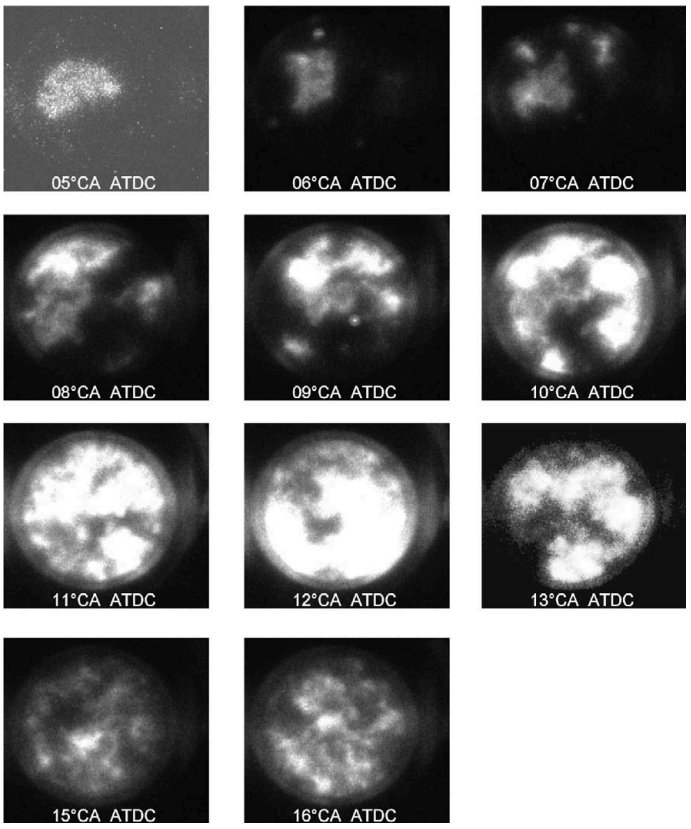

Figure 16: Chemiluminescence pictures (308 nm); spark plug-assisted HCCI; (experimental setup II); image size: 14 x 14 cm; λ = 2.8; time: -25° CA BTDC

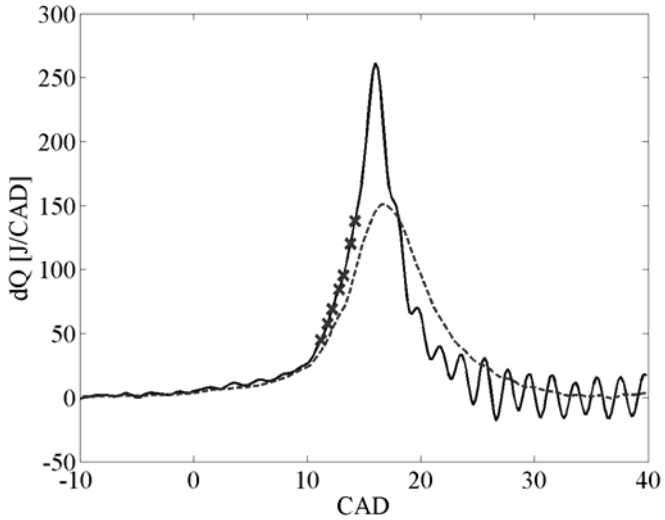

Figure 17: Heat release; spark plug-assisted HCCI; λ = 2.8; ignition time: -25° CA BTDC; solid line corresponds to the PLIF picture series in Fig. 5; dots indicate the CAD when the PLIF pictures are taken; dashed line: average of 100 cycles, 50 taken before and 50 after the heat release indicated by the solid line

CONCLUSION

The effect of spark plug and laser plasma ignition on the ignition timing of a research engine running in HCCI mode was investigated. The fuel used in these experiments consisted of a mixture of 80 % isooctane and 20 % n-heptane. The engine allowed comprehensive optical diagnostics by different laser spectroscopic, optical and imaging techniques in addition to the standard monitoring devices like pressure transducers and exhaust gas analysis. Unlike in the case of methane, where the effect of laser ignition on the HCCI process was evident in the pressure and heat release curves [7], the influence of additional ignition sources on a mixture with easier autoignition properties like n-heptane is more subtle. The heat release curves show no significant effect on the overall performance of the engine whether unsupported HCCI or spark/laser-assisted mode were investigated because the cycle-to-cycle have been too large. But the optical diagnostics reveal that, beginning at the ignition point, a flame structure develops and propagates in the first CAD in a way similar to conventional SI engines. This indicates that when using other fuels than n-heptane being less prone to autoignition like isooctane or gasoline, the effect of laser or spark plug ignition on the combustion rate or ignition timing can be expected to be more pronounced like in the case of methane. Another explanation to the weak effect of either method of support could be that the HCCI combustion starts at the walls in this particular engine [1] and thus the ignition source that would heat up the charge and advance the auto-ignition timing should be placed closer to the cylinder wall. The obvious difference in the flame development between unsupported and laser or spark plug supported HCCI having been observed by different imaging techniques emphasize the value of additional diagnostic techniques together with standard engine diagnostics.

ACKNOWLEDGMENTS

Financing by GE Jenbacher GmbH & Co OHG, Austria, and by the European Community IHP program “Access to Research Infrastructure” through contract number HPRI-CT-2001-00166 (FP-5), is gratefully acknowledged.

REFERENCES

1. A. Hultqvist, M. Christensen, B. Johansson, A. Franke, M. Richter, M. Aldén: “A Study of the Homogeneous Charge Compression Ignition Combustion Process by Chemiluminescence Imaging”, SAE1999-01-3680
2. M. Christensen, B. Johansson: ”Influence of Mixture Quality on Homogeneous Charge Compression Ignition”, SAE9824541
3. T. Aoyama, Y. Hattori, J. Mizuta, Y. Sato: ”AnExperimental Study on a Premixed-Charge Compression Ignition Gasoline Engine, SAE960081
4. J-O. Olsson, O. Erlandsson, B. Johansson: ”Experiments and Simulation of a Six-Cylinder Homogeneous Charge Compression Ignition (HCCI) Engine”, SAE2000-01-2867
5. S. Onishi, S. Hong Jo, K. Shoda, P. Do Jo, S. Kato: ”Active Thermo-Atmosphere Combustion (ATAC) – A New Combustion Process for Internal Combustion Engines”, SAE790501
6. R.H. Thring: ”Homogeneous-Charge Compression-Ignition (HCCI) Engines”, SAE892068
7. H. Kopecek, E. Wintner, M. Lackner, F. Winter, A. Hultqvist: “Laser-stimulated Ignition in a Homogeneous Charge Compression Ignition Engine”, SAE2004-01-0937
8. M. Christensen, A. Hultqvist, B. Johansson: “Demonstrating the Multi Fuel Capability of a Homogeneous Charge Compression Ignition Engine with Variable Compression Ratio”,SAE1999-01-3679
9. M. Christensen, P. Einewall, B. Johansson: ”Homogeneous Charge Compression Ignition (HCCI) Using Iso-octane, Ethanol and Natural Gas-A Comparison to Spark Ignition Operation”, SAE972874
10. J-O. Olsson, P. Tunestal, B. Johansson: ” Closed-Loop Control of an HCCI Engine”, SAE2001-01-1031
11. J-O. Olsson, P. Tunestal, G. Haraldsson, B. Johansson: ”A Turbo Charged Dual Fuel HCCI Engine”, SAE2001-01-1896
12. O. Erlandsson, B. Johansson, F. A. Silversand: ”Hydrocarbon (HC) Reduction of Exhaust Gases from a Homogeneous Charge Compression Ignition (HCCI) Engine Using Different Catalytic Mesh-Coatings”, SAE2000-01-1847
13. D. Law, J. Allen, D. Kemp, G. Kirkpatrick, T. Copland: “Controlled Combustion in an IC-Engine with a Fully Variable Valve Train”, SAE 2001 World Congress, March 2001, Detroit, MI, USA
14. P.D. Ronney: “Laser versus conventional ignition of flames”, Opt. Eng. **33** (2), 510-521, 1994.
15. F.J. Weinberg, J.R. Wilson: “A Preliminary Investigation of the Use of Focused Laser Beams for Minimum Ignition Energy Studies”, Proc. Roy. Soc. London, A **321**, 41-52, 1971.
16. H. Kopecek, H. Maier, G. Reiser, F. Winter, E. Wintner: „Laser Ignition of Methane-Air mixtures at High Pressures“, Experimental Thermal and Fluid Science **27**, 499-503, 2003.
17. M. Weinrotter, H. Kopecek, M. Tesch, M. Lackner, F. Winter, E. Wintner: “Laser ignition of ultra-lean methane-hydrogen-air and hydrogen-air mixtures under engine-like conditions”, Experimental and Thermal fluid science, article in press.
18. J.D. Dale, P.R. Smy, R.M. Clements: “Laser Ignited Internal Combustion Engine – An Experimental Study”, SAE-780329, Detroit, 1978.
19. H. Kopecek, S. Charareh, M. Lackner, C. Forsich, F. Winter, J. Klausner, G. Herdin, E. Wintner: „Laser Ignition of Methane-Air Mixtures at High Pressures

and Diagnostics“, ASME, ICES2003-614, Austria, 2003.
20. M. Weinrotter, H. Kopecek, M. Lackner, F. Winter, E. Wintner: “Application of Laser Ignition to Hydrogen-Air Mixtures at High Pressures”, International Journal of Hydrogen Energy, article in press.
21. C.F. Kaminski, J. Hult, M. Aldén, Appl Phys B **68**, 757-760, 1999.
22. C.F. Kaminski, J. Hult, M. Aldén, S. Lindenmaier, A. Dreizler, U. Maas, M. Baum, In Twenty-Eight Symposium (International) on Combustion, The Combustion Institute, Pittsburgh, 399-405, 2000.
23. J. Hult, M. Richter, J. Nygren, M. Aldén, A. Hultqvist, M. Christensen, B. Johansson, Appl. Optics B 41, 5002-5014, 2002.
24. J. Graf, M. Weinrotter, H. Kopecek, E. Wintner, Laser Ignition, Optics and Contamination of Optics in an I.C. Engine. ASME Internal Combustion Engine Division, Fall Technical Conference, ICEF2004-833, USA, 2004.

CONTACT

Martin Weinrotter, Vienna University of Technology, Photonics Institute, Gusshausstrasse 27, 1040 Wien, Austria, email: martin.weinrotter@tuwien.ac.at

DEFINITIONS, ACRONYMS, ABBREVIATIONS

HCCI Homogeneous Charged Compression Ignition

Nd:YAG Neodymium Yttrium Aluminum Garnet

PLIF Planar Laser-Induced Fluorescence

TDC Top Dead Center

EGR Exhaust Gas Recirculation

IMEP Indicated Mean Effective Pressure

NO_x The sum of nitrogen oxides

SI Spark Ignition

BBDC Before Bottom Dead Center

ABTD After Bottom Dead Center

BTDC Before Top Dead Center

ATDC After Top Dead Center

λ Relative air-fuel ratio

CAD Crank Angle Degree

MCP Micro Channel Plate

COV Coefficient of Variation